Article

Assessment of Contamination Management Caused by Copper and Zinc Cations Leaching and Their Impact on the Hydraulic Properties of a Sandy and a Loamy Clay Soil

Anastasia Angelaki [1,*], Alkiviadis Dionysidis [1], Parveen Sihag [2,3] and Evangelia E. Golia [4,5]

1. Laboratory of Agricultural Hydraulics, Department of Agriculture, Crop Production and Rural Environment, University of Thessaly, Fytokou Street, 384 46 Volos, Greece; adionysid@uth.gr
2. Department of Civil Engineering, University Institute of Engineering, Chandigarh University, Mohali 140413, India; parveen.e11725@cumail.in or parveen12sihag@gmail.com
3. University Centre for Research & Development, Chandigarh University, Mohali 140413, India
4. Laboratory of Soil Science, Department of Agriculture, Crop Production and Rural Environment, University of Thessaly, Fytokou Street, 384 46 Volos, Greece; egolia@auth.gr
5. Laboratory of Soil Science, School of Agriculture, Aristotle University of Thessaloniki, 541 24 Thessaloniki, Greece
* Correspondence: anaggel@uth.gr; Tel.: +30-242-109-3061

Abstract: Soil hydraulic properties are crucial to agriculture and water management and depend on soil structure. The impact of Cu and Zn cations on the hydraulic properties of sandy and loamy clay soil samples of Central Greece, was investigated in the present study. Metal solutions with increased concentrations were used to contaminate the soil samples and the effect on hydraulic properties was evaluated, demonstrating the innovation of the current study. The soil samples were packed separately into transparent columns and the initial values of hydraulic conductivity, cumulative infiltration, infiltration rate and sorptivity were estimated. In order to evaluate soil adsorption, metal concentrations were measured at the water leachate. After the contamination of the soil samples, the hydraulic properties under investigation were determined again, using distilled water as the incoming fluid; the differences at the hydraulic parameters were observed. After doubling metal concentrations into the incoming solution of loamy clay soil, metal adsorption and the values of the hydraulic parameters increased significantly. Loamy clay soil showed interaction between the clay particles and the positive charge in the incoming fluid, which led to a possible increase in aggregation. Furthermore, aggregation may led to pore generation. Contamination of sandy soil exhibited no impact on aggregation and soil structure. In order to evaluate the differences on the hydraulic properties and soil structure, the experimental points were approximated with two infiltration models.

Keywords: hydraulic conductivity; sorptivity; infiltration; heavy metals; irrigation; pollution

1. Introduction

Soil hydraulic properties strongly influence agricultural and environmental applications, due to their significant role in irrigation, drainage, water balance, nutrient leaching provision, water supply to crops [1]. Soil structure and soil porosity determine the hydraulic properties of the soil [2]. Hydraulic conductivity is a very important parameter in irrigation planning, as it is related to models that predict infiltration and to other hydraulic parameters, such as sorptivity, diffusivity and capacity. Hydraulic conductivity expresses the ability of water to move through soil, it is equal to the velocity of water and it affects soil water dynamics, evapotranspiration and irrigation [3–6]. Cumulative infiltration along with infiltration rate through the soil affects the water cycle, evapotranspiration, runoff, floods, aquifer recharge, irrigation, and the environment in general. Climate change affects

the infiltration process. Climate change reacts on precipitation, affecting evapotranspiration, runoff and infiltration rates. Designing an irrigation network is directly related to infiltration, because of the impact on the hydraulic parameters [7,8]. Field capacity is linked to soil moisture; it depends on the soil texture/structure [9]. Infiltration is also influenced by various physical soil properties, such as soil structure and texture, soil moisture, density, sorptivity, hydraulic conductivity, diffusivity, capacity, etc. [10]. The infiltration rate is high at the start of the phenomenon, when the soil is unsaturated; it gradually reduces, reaching a constant value. Knowledge of the exact mechanism is necessary for reaching a high level of irrigation management [11]. Thus, decoding infiltration mechanism and how it is influenced by the constitution of the incoming fluids and the quality of the soil types is crucial to irrigation planning and water management. However, the design and the accomplishment of an infiltration experimental procedure is always challenging [12]. Evaluation of infiltration is multiplicative due to spatio-temporal distribution [13]. Many researchers have worked on the estimation of soil properties via infiltration data [10,14–19].

Green & Ampt [20] proposed one of the most popular models for cumulative infiltration, considering of a homogenous soil column with known initial moisture, which is constant throughout the column and with ponding conditions on soil surface. Green & Ampt (G&A) model is given in Equation (1):

$$K_s t = I - \frac{S^2}{2K_s} ln\left(1 + \frac{2K_s}{S^2}I\right) \tag{1}$$

where K_s is hydraulic conductivity at saturation, t is time, I is cumulative infiltration and S is sorptivity of the soil and is given below (Equation (2)):

$$S^2 = 2K_s(\theta_i - \theta_o)\left(H_o - H_f\right) \tag{2}$$

where $K_s(z,t)$ is the saturated hydraulic conductivity, θ_o is the initial moisture of the soil, θ_i is the boundary water content, H_o is the hydraulic load at the surface of the column and H_f is the pressure at the wet front.

Starting from the Richards [21] equation for vertical one dimensional water flow:

$$\frac{\partial \theta}{\partial t} = \frac{\partial}{\partial z}\left(D\frac{\partial \theta}{\partial z}\right) - \frac{\partial K}{\partial z} \tag{3}$$

Parlange [22] proposed his two parametric model (P), shown in Equation (4):

$$K_s t = I + \frac{S^2}{2K_s}\left[exp\left(-\frac{2K_s}{S^2}I\right) - 1\right] \tag{4}$$

where K_s is hydraulic conductivity at saturation, t is time, I is cumulative infiltration and S is soil sorptivity.

As sorptivity and hydraulic conductivity are two of the most important hydraulic parameters, their presence in infiltration mathematical models is significant. As shown above, they are evolved in the most important infiltration models, such as Green & Ampt, and Parlange's model [23–26].

At the early phase of infiltration, when capillary forces overcome gravity, Green & Ampt, Parlange and Philip's infiltration models, converge to Equation (5):

$$I = St^{1/2} \tag{5}$$

where I indicates the cumulative infiltration, S is sorptivity and t denotes the time [26].

The infiltration process often occurs in the field, when the incoming water contains heavy metal cations (e.g., Cu and Zn), which is very common in treated municipal wastewater, fertilizers, or appear in polluted influents due to flood incidents near industrial areas or landfill, adjacent to agricultural fields [27–29]. In cultivated soils, Cu content and ap-

plication rate, which are to blame for the copper inputs in agricultural soils, differs across various agricultural materials [30]. Pesticides, fertilisers, manure, wastewaters and mineral are the most often sources of copper input in soils of cultivated areas [31,32], but traffic contributes to local Cu inputs, too. On the other hand, Zn inputs are often related to agricultural practices, fertilisers, atmospheric depositions and wastewater application [28,32]. The application of fertilizers with anions (such as phosphates) and cations (such as metals) usually decrease aggregates stability and enhance soil erosion through increasing charge density of particle soil surfaces. Aggregation, dispersion and charging of soil solution is highly affected by mainly divalent cations along with soil pH and ionic strength [27,28,30]. Adsorption of Zn onto solid phases occurs quickly, just after the contact of Zn with soil [33]. Conditionally, heavy metals can be valuable and beneficial to crops, but their toxic impact is important if the concentrations transcend specific limits [34].

Bourazanis et al. [35] focused on the effect of certain parameters and elements of treated municipal wastewaters on saturated hydraulic conductivity of undisturbed soils samples, while Markiewicz-Patkowska et al. [36] researched on the sorption behaviour of Cu and Zn, among others, at different values of pH. In acidic soils, the availabilityand solubility of Zn^{2+} ions are higher than in alkaline. Nartowska et al. [37] investigated the impact of Cu and Zn on the microstructural parameters and the hydraulic conductivity of bentonites, showing that Cu ions increased hydraulic conductivity; the Kozlowski et al. [38] formula can be used in order to estimate hydraulic conductivity, when bentonites are contaminated with Cu. In contrast, the behaviour of bentonites contaminated with Zn is similar to the physical parameters of clay.

Soil structure exerts important influences on the soil conditions and the environment [39]. It is often expressed as the degree of the stability of aggregates. Clay minerals shows high physical and chemical adsorption capacity, due to soil particles with negative charge and large surface [40]. Contrariwise to sandy soil, clay's unique mineralogy (pore structure, pore size and porosity) should be considered when investigating the adsorpability [39,40] gap [30,41]. The amount and the type of clay minerals in the soil, along with soil pH, organic matter and the presence of cations (e.g., Cu^{+2} and Zn^{+2}) in drainage solution is essential to aggregate formation and soil health [27]. Clay minerals are abundant minerals in soils. Siallitic weathering under cooler climate conditions yields smectite minerals, which are characterized by a high adsorption capacity due to their negative layer charge, whereas allitic weathering occurring under tropic conditions yields aluminium hydroxides that do not carry a permanent surface charge. Crop productivity is related to aggregation of the soil; low aggregated soils show low crop productivity, while well-aggregated soils lead to greater crop productivity, are not so sensitive to erosion, and affect carbon sequestration [39].

Although it has been noted that soil aggregation is related to heavy metal concentrations [42–44], information about the adsorption/desorption and the distribution of heavy metals at soil aggregation is still rare [45]. In addition, although some researchers have lately worked on physicochemical properties at different soil types and different land uses (e.g., [46,47]), there is a knowledge gap; it is a research challenge to investigate the direct effect of the heavy metals on soil's hydraulic properties, which are influential to infiltration, drainage, runoff, aquifer recharge and irrigation planning. The main aim of this work was to investigate the impact of Cu and Zn solutions with increased concentrations on hydraulic conductivity, infiltration, sorptivity and infiltration rate of sandy and loamy clay soil samples. In addition, in order to evaluate the differences on the hydraulic properties and soil structure, the experimental points were approximated with G&A and P models.

2. Materials and Methods

The study was set up and implemented at the Laboratory of Agricultural Hydraulics and the Laboratory of Soil Science at the Department of Agriculture, Crop Production and Rural Environment, School of Agricultural Sciences, University of Thessaly, Volos, Greece. In order to obtain contrary soil textures, two locations were selected: The Farm of the Department of Agriculture, Crop Production & Rural Environment of University of

Thessaly, Velestino, Greece (latitude 39°22′43″ N, longitude 22°44′30″ E, altitude 70 m above sea level) and the riverside of Anavros, Volos, Greece (latitude 39°21′01.04″ N, longitude 22°57′47.17″ E, altitude 3 m above sea level). We used two soil samples (with two replicates) consisting of eight subsamples each, spread evenly across an area of 10 m² using a zig-zag sampling pattern. The two soil samples were collected at 0–15 cm depths and were analyzed as follows: soil pH and electrical conductivity (EC) was measured in deionized water with a soil solution ratio of 1:1 [48]. Particle size distribution was measured using Bouyoucos hydrometer [49]. Soil organic matter was measured using the Walkley–Black method [49]. "Pseudo-total" potentially harmful metals concentrations were measured according to the modified BCR method using aqua regia (with HCl:HNO$_3$ 3:1) and after 2 h digestion [48,50,51]. The concentrations of all the metals studied were determined by atomic absorption spectrophotometry (AAS) using the flame (F-AAS) or the graphite furnace (GF) techniques [52,53] according to their detection limits. The concentrations of copper and zinc in the initial and outgoing solutions were measured by making the required dilutions. In some cases, the standard addition method was used.

The soil samples were screened using Octagon 2000 sieve shaker, consisting of 6 sieves with 2.00 mm, 1.00 mm, 500 μm, 250 μm, 106 μm and 33 μm mesh diameters. After sieving the soils, the big particles (staying on 2.00 mm sieve) and the very small ones (passing through the 33 μm sieve) were excluded. The experiment was performed in two replications, so two identical columns were set up in the laboratory and were filled in the same way for each soil sample. The soil samples were placed in the oven at 105 °C for 24 h and each was packed uniformly into two identical columns of plexiglas with inner diameter 6 cm. Uniformity was achieved using a PVC column equipped with sieves. Soil passed through the sieves before entering the plexiglas column and touched the surface of the soil, keeping constant the distance between the PVC and the soil surface. The procedure constitutes an effective method to achieve good distribution of the soil column. In order to estimate hydraulic conductivity at saturation (K_s), the constant head method was used [54] for both soil samples (with two replicates each). This method is based on Darcy's law application to a one-dimensional constant flow into a saturated soil column [55]. The length of each soil column was L = 15 cm, the soil surface was A = 28.26 cm² and the pressure head on the soil surface was ΔH = 3 cm.

In order to record cumulative infiltration data, a second round of experiments was carried out, by using each soil sample to fill two plexiglas columns with a 6 cm diameter and 1 m length each. At the top of each column, a flexible tube was adapted, in order to act as outflow helping to achieve a steady head of about 2 mm above the soil surface. The cumulative volumes of the incoming water (distilled) were calculated by subtracting the outflow volumes from the incoming volumes of the fluid. The incoming water was recorded every minute at the sandy soil sample and every two minutes at the loamy clay soil, simulating irrigation under ponding conditions in the laboratory (two replicates). Subsequently, solutions of Cu 200 mg·L⁻¹ (Cu 200), Cu 400 mg·L⁻¹ (Cu 400), Zn 200 mg·L⁻¹ (Zn 200) and Zn 400 mg·L⁻¹ (Zn 400) were used as incoming solutions at both soil columns, respectively. Conclusively, the following experimental design was conducted: 2 soil samples × 2 replicates each × 5 metal concentrations (0 mg·L⁻¹, 200 Cu 200 mg·L⁻¹ (Cu 200), Cu 400 mg·L⁻¹ (Cu 400), Zn 200 mg·L⁻¹ (Zn 200) and Zn 400 mg·L⁻¹ (Zn 400)). Cu and Zn solutions were prepared from standard NIST Certipur Cu(NO$_3$)$_2$ and Zn (NO$_3$)$_2$ 1000 mg·L⁻¹ Cu or Zn (in HNO$_3$ 0.5 mol·L⁻¹), after proper dilutions. The concentrations of Cu and Zn cations were also measured in the outgoing water at all cases. Adsorption was estimated by subtracting the concentrations at the outgoing fluid from the ones at the initial fluid.

After the contamination of the soil samples, distilled water was used again as the incoming fluid and the hydraulic properties under investigation were determined again.

The SPSS (version 26.0) software was used in order to conduct the statistical procedure. One-way analysis of variance (ANOVA) was used in order to check the data using the LSD test of $p < 0.05$ significant level. The arithmetic average values along with the standard deviation and relative standard deviation of PHMs concentrations were calculated to

describe the data variation. Two replicates for each data values were averaged prior to the statistical analyses.

3. Results

The two soil samples under investigation, according to soil characterization protocol, were characterized sandy (S) and loamy clay (LC) soils. Table 1 shows the chemical and physical properties of the soil samples.

Table 1. Chemical and physical properties of the soil samples (*n* = 5).

	S	LC
pH	7.4 ± 0.38 *	7.6 ± 0.4
Organic C (%)	0.3 ± 0.1	5.1 ± 0.3
Clay (%)	13 ± 0.9	58 ± 0.9
Sand (%)	61 ± 0.9	17 ± 0.8
Bulk density ρ_b (g·cm^{-3})	1.60 ± 0.12	1.32 ± 0.10
Total Cu (mg/kg dry soil)	ND **	ND
Total Zn (mg/kg dry soil)	ND	ND

* RSD (Relative Standard Deviation); ** ND: Not Detectable.

The concentrations of Cu and Zn cations were measured at the water leachate at all cases. Adsorption (A_1) was estimated by subtracting the concentrations at the outgoing fluid from the ones of the initial fluid. Adsorption was re-calculated (A_2), after doubling the initial concentration (singly for Cu and Zn). The % difference between the two values of soil adsorption was calculated using the following formula:

$$\frac{|A_1 - A_2|}{A_1} \cdot 100\%$$ (6)

It should be noted that all the results presented below, are the average of the two experimental repetitions that took place for each soil sample. Table 2 shows the percentage average increase in the cumulative infiltration values after contaminating the soil samples with Cu 200, Cu 400, Zn 200 and Zn 400 solutions.

Table 2. Percentage of average increase at cumulative infiltration, after contaminating with Cu 200 mg·L^{-1} solution (Cu 200), after contaminating with Cu 400 mg·L^{-1} solution (Cu 400), after contaminating with Zn 200 mg·L^{-1} solution (Zn 200) and after contaminating with Zn 400 mg·L^{-1} solution (Zn 400), for sandy (S) and loamy clay (LC) soil (*n* = 2).

|	S	LC
	% Average Increase at Cumulative Infiltration	% Average Increase at Cumulative Infiltration
initial-after Cu 200	1.100 ± 0.005	12.900 ± 0.008
initial-after Cu 400	1.100 ± 0.014	35.500 ± 0.006
after Cu 400-after Cu 200	0.100 ± 0.005	**19.900** ± 0.050
initial-after Zn 200	0.700 ± 0.029	12.300 ± 0.008
initial-after Zn 400	0.700 ± 0.014	15.500 ± 0.013
after Zn 400-after Zn 200	0.040 ± 0.013	**3.100** ± 0.097

Hydraulic conductivity at saturation was increased by 20% and 3% in the cases of Cu and Zn solutions respectively (Table 3). Derivative dI/dt at late times of infiltration is equal to infiltration rate and tends to K_s at both soil samples and at all solution cases, confirming good monitoring of the experiments [10]. The dI/dt values increased 20% and 2.7% after doubling the Cu and Zn concentrations, respectively, at loamy clay soil (Table 3).

Table 3. Hydraulic conductivity (K_s) and derivative dI/dt at late times of infiltration, initial (before contaminating the soil column with the Cu and Zn solutions), after contaminating with Cu 200 mg·L^{-1} solution (Cu 200), after contaminating with Cu 400 mg·L^{-1} solution (Cu 400), after contaminating with Zn 200 mg·L^{-1} solution (Zn 200) and after contaminating with Zn 400 mg·L^{-1} solution (Zn 400), for sandy (S) and loamy clay (LC) soil (n = 2).

	S			LC		
	K_s (cm/min)	dI/dt (cm/min)	mse (K_s-dI/dt)	K_s (cm/min)	dI/dt (cm/min)	mse (K_s-dI/dt)
Initial	0.820 ± 0.006	0.800 ± 0.003	0.0004	0.049 ± 0.010	0.050 ± 0.010	0.000001
After Cu 200	0.890 ± 0.011	0.880 ± 0.017	0.0001	0.090 ± 0.011	0.100 ± 0.005	0.000100
After Cu 400	0.890 ± 0.011	0.880 ± 0.011	0.0001	0.108 ± 0.005	0.120 ± 0.008	00.00025
After Zn 200	0.820 ± 0.012	0.830 ± 0.006	0.0001	0.070 ± 0.014	0.075 ± 0.013	0.000025
After Zn 400	0.820 ± 0.009	0.830 ± 0.012	0.0001	0.072 ± 0.007	0.077 ± 0.007	0.000025
mse (initial-after Cu 200)	0.0049	0.0064		0.0017	0.0025	
mse (initial-after Cu 400)	0.0049	0.0064		0.0004	0.0006	
mse (initial-after Zn 200)	0.0000	0.0009		0.0035	0.0049	
mse (initial-after Zn 400)	0.0000	0.0009		0.0005	0.0007	
% increase (after Cu 400-after Cu 200)	0.0	0.0		**20.0 ± 1.0**	**20.0 ± 1.0**	
% increase (after Zn 400-after Zn 200)	0.0	0.0		**3.0 ± 0.6**	**2.7 ± 0.5**	

Figure 1 shows the cumulative infiltration I(t) curves for sandy soil (S) at 5 cases: (a) the initial curve (before contaminating the soil column with the Cu and Zn solutions) (b) after contaminating with Cu 200 mg·L^{-1} solution (Cu 200) (c) after contaminating with Cu 400 mg·L^{-1} solution (Cu 400) (d) after contaminating with Zn 200 mg·L^{-1} solution (Zn 200) and (e) after contaminating with Zn 400 mg·L^{-1} solution (Zn 400). In Figure 2, the cumulative infiltration versus time for loamy clay soil (LC) is shown, for the same 5 cases as above. Figure 3 illustrates collectively cumulative infiltration curves for loamy clay soil (LC), where (a) shows the initial (before contaminating the soil column with the Cu and Zn solutions), the after contamination with Cu 200 mg·L^{-1} solution (Cu 200) and after contamination with Cu 400 mg·L^{-1} solution (Cu 400) infiltration curve and (b) shows the initial (before contaminating the soil column with the Cu and Zn solutions), the after contamination with Zn 200 mg·L^{-1} solution (Zn 200) and the after contamination with Zn 400 mg·L^{-1} solution (Zn 400) cumulative infiltration curve.
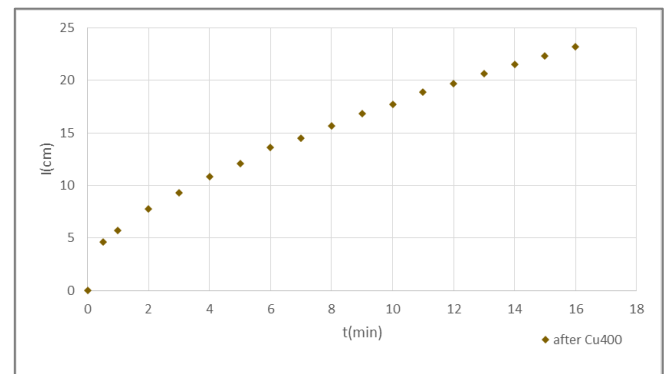
In Figures 4 and 5 cumulative infiltration vs. square root of time for sandy (S) and loamy clay (LC) soil is shown respectively, for the 5 cases: (a) initial, (b) after Cu 200, (c) after Cu 400, (d) after Zn 200 and (e) after Zn 400 contamination of the soil samples. I($t^{1/2}$) functions show the relations between the infiltration (I) and the square root of time ($t^{1/2}$) at the early times of the phenomenon, where the slope is equal to sorptivity of the soil (Equation (2)). At early times in the infiltration process, capillary forces are stronger than gravity [10]. Sorptivity (S) values for both soil samples and all cases are given in Table 4, where, in loamy clay soil, after doubling the concentration of copper in the incoming solution, a 20% increase in soil sorptivity was indicated. In addition, a 2.2% increase in sorptivity was mentioned in the case of Zn.
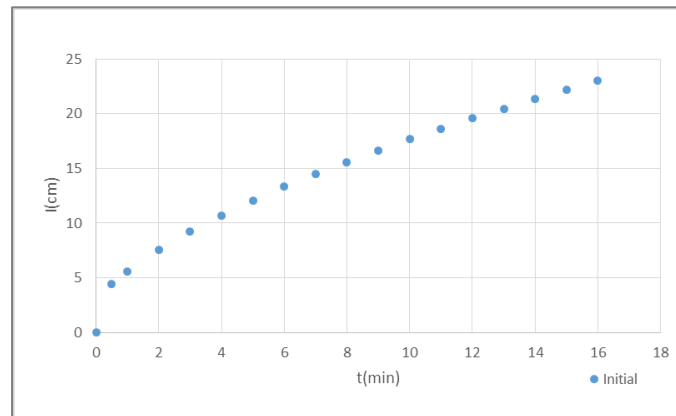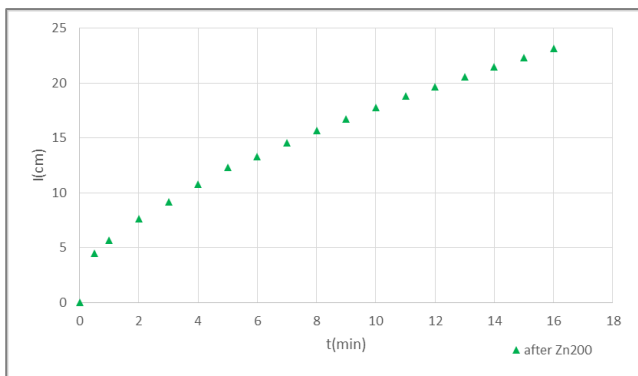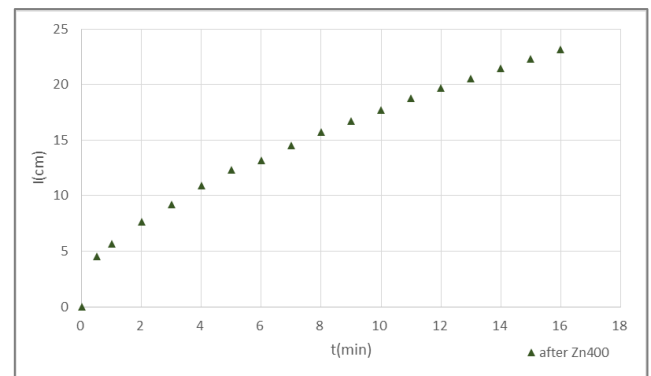
(**a**)
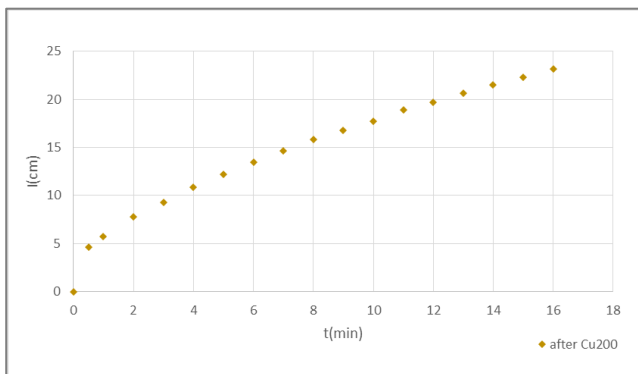
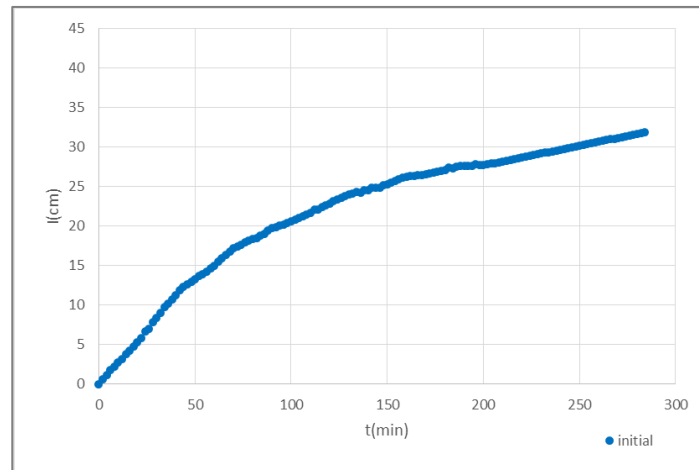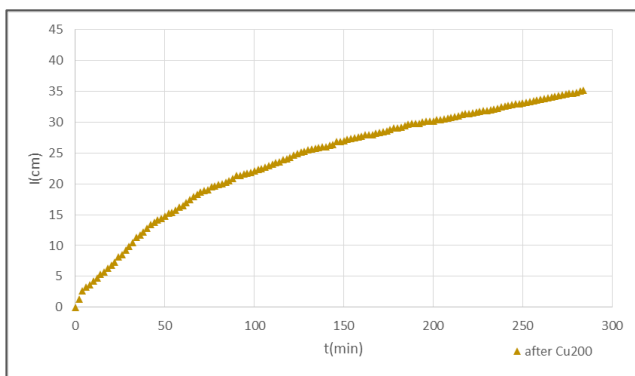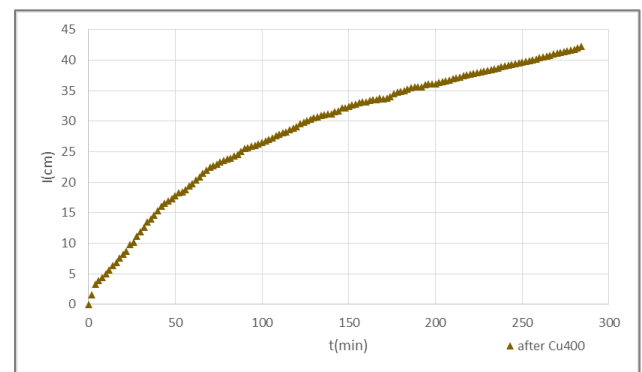(**b**)

(**c**)

(**d**)

(**e**)

Figure 1. Cumulative infiltration versus time for sandy soil (S) (**a**) initial (before contaminating the soil column with the Cu and Zn solutions) (**b**) after contaminating with Cu 200 mg·L^{-1} solution (Cu 200) (**c**) after contaminating with Cu 400 mg·L^{-1} solution (Cu 400) (**d**) after contaminating with Zn 200 mg·L^{-1} solution (Zn 200) (**e**) after contaminating with Zn 400 mg·L^{-1} solution (Zn 400) (*n* = 2).
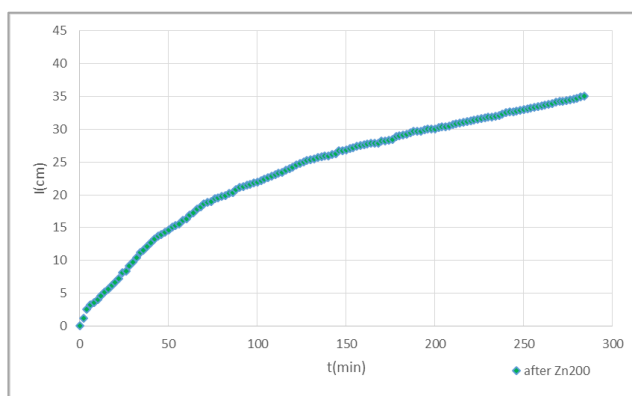
(**a**)

(**b**)

(**c**)

(**d**)

(**e**)
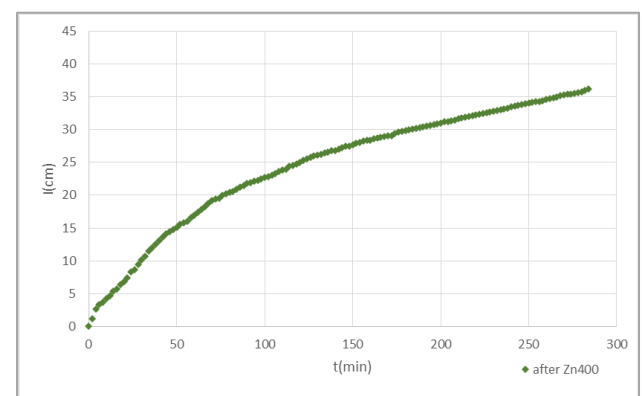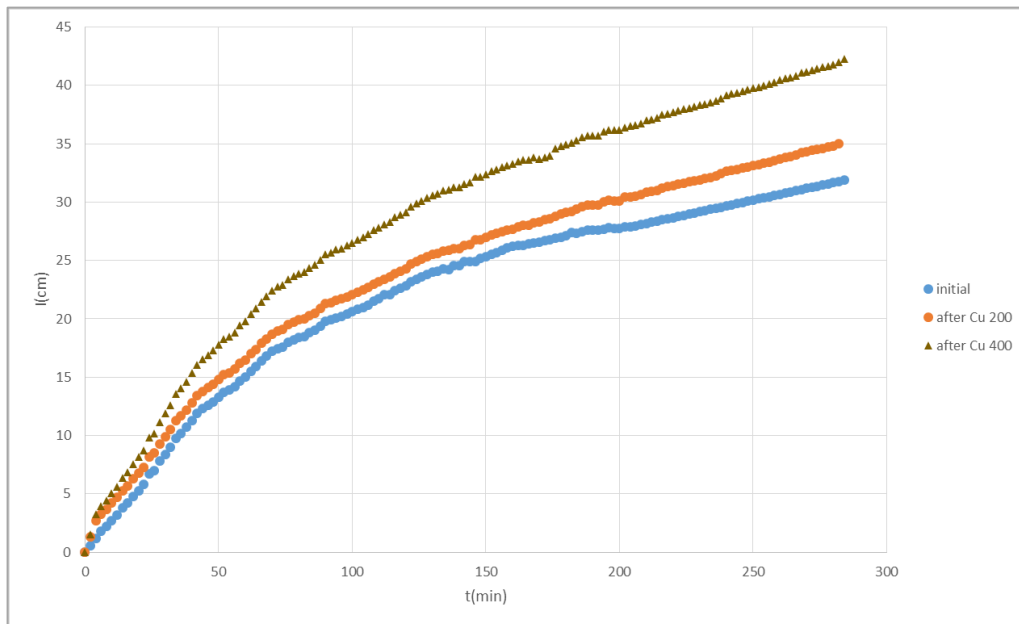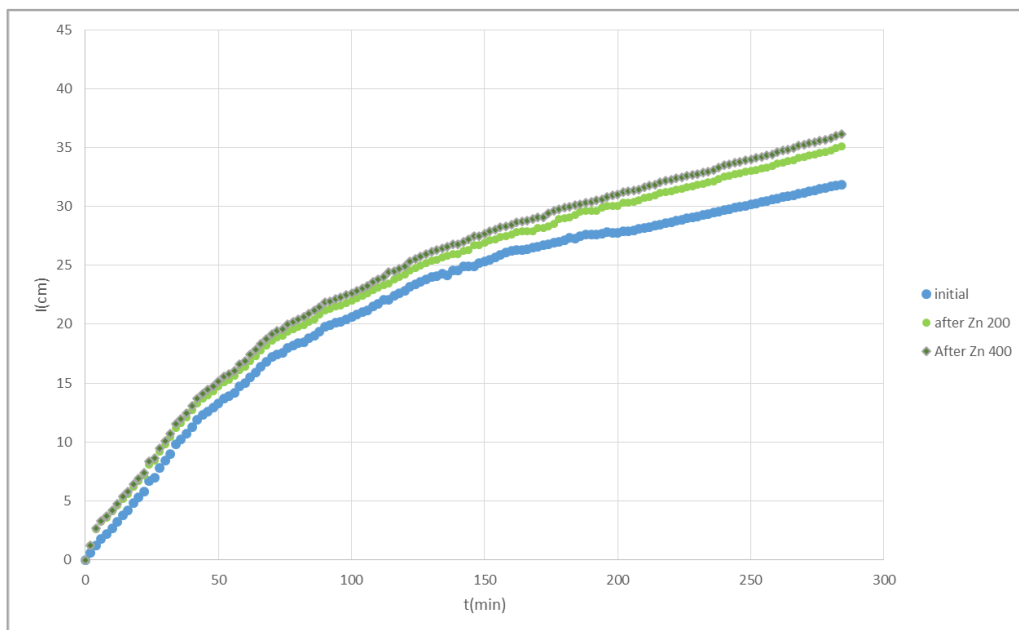
Figure 2. Cumulative infiltration versus time for loamy clay soil (LC) (**a**) initial (before contaminating the soil column with the Cu and Zn solutions) (**b**) after contaminating with Cu 200 mg·L^{-1} solution (Cu 200) (**c**) after contaminating with Cu 400 mg·L^{-1} solution (Cu 400) (**d**) after contaminating with Zn 200 mg·L^{-1} solution (Zn 200) (**e**) after contaminating with Zn 400 mg·L^{-1} solution (Zn 400) (*n* = 2).
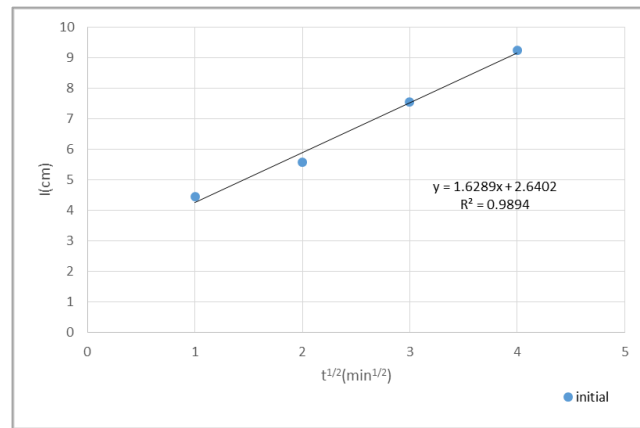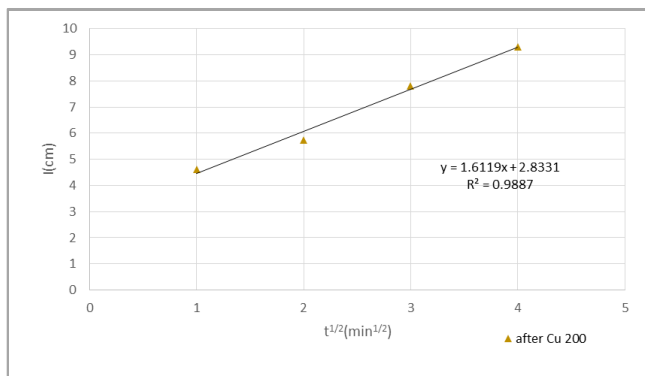
(**a**)

(**b**)

Figure 3. Comparison of cumulative infiltration versus time for loamy clay soil (LC) between: (**a**) initial (before contaminating the soil column with the Cu and Zn solutions), after contamination with Cu 200 mg·L^{-1} solution (Cu 200) and after contamination with Cu 400 mg·L^{-1} solution (Cu 400) (**b**) initial (before contaminating the soil column with the Cu and Zn solutions), after contamination with Zn 200 mg·L^{-1} solution (Zn 200) and after contamination with Zn 400 mg·L^{-1} solution (Zn 400) ($n = 2$).

(**a**)

(**b**)

(**c**)
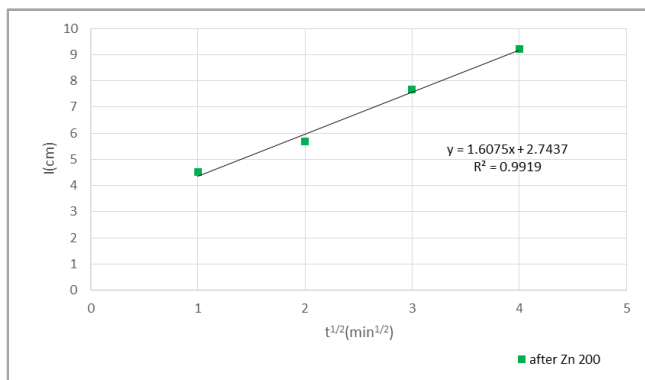
(**d**)
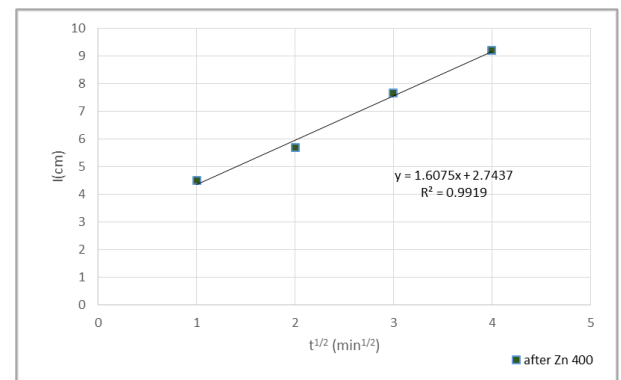
(**e**)

Figure 4. Cumulative infiltration versus square root of time for sandy soil (S) (**a**) initial (before contaminating the soil column with the Cu and Zn solutions) (**b**) after contaminating with Cu 200 mg·L^{-1} solution (Cu 200) (**c**) after contaminating with Cu 400 mg·L^{-1} solution (Cu 400) (**d**) after contaminating with Zn 200 mg·L^{-1} solution (Zn 200) (**e**) after contaminating with Zn 400 mg·L^{-1} solution (Zn 400) ($n = 2$).
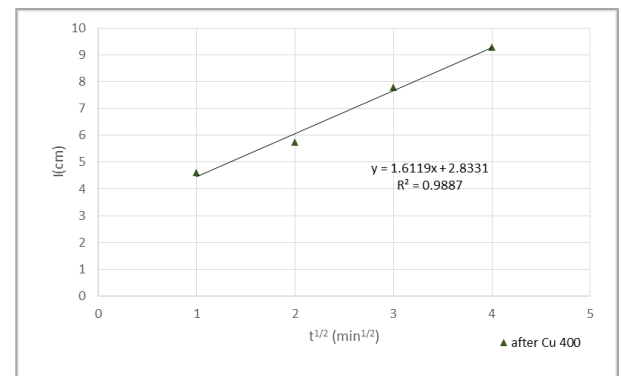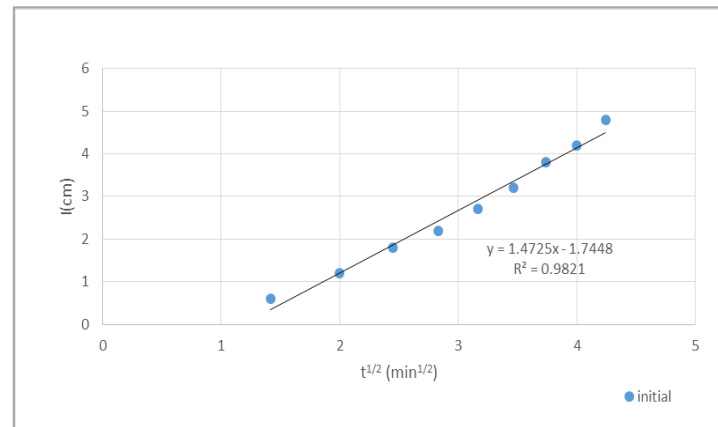
(**a**)
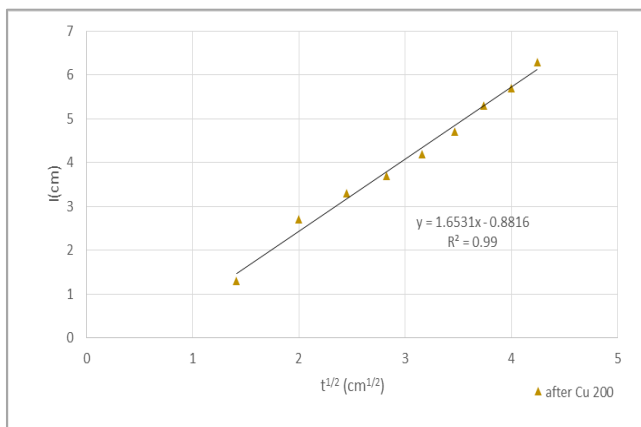
(**b**)
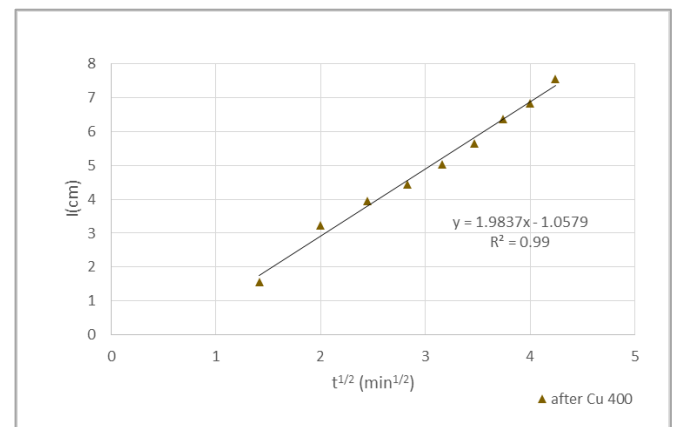
(**c**)

(**d**)

(**e**)

Figure 5. Cumulative infiltration versus square root of time for loamy clay soil (LC) (**a**) initial (before contaminating the soil column with the Cu and Zn solutions) (**b**) after contaminating with Cu 200 mg·L^{-1} solution (Cu 200) (**c**) after contaminating with Cu 400 mg·L^{-1} solution (Cu 400) (**d**) after contaminating with Zn 200 mg·L^{-1} solution (Zn 200) (**e**) after contaminating with Zn 400 mg·L^{-1} solution (Zn 400) (*n* = 2).

Table 4. Sorptivity (S), initial (before contaminating the soil column with the Cu and Zn solutions), after contaminating with Cu 200 mg·L^{-1} solution (Cu 200), after contaminating with Cu 400 mg·L^{-1} solution (Cu 400), after contaminating with Zn 200 mg·L^{-1} solution (Zn 200) and after contaminating with Zn 400 mg·L^{-1} solution (Zn 400), for sandy (S) and loamy clay (LC) soil (*n* = 2).

	S	LC
	S (cm/min$^{1/2}$)	S (cm/min$^{1/2}$)
Initial	4.6754 ± 0.0001	1.4725 ± 0.0007
After Cu 200	4.6315 ± 0.0002	1.6531 ± 0.0003
After Cu 400	4.6315 ± 0.0003	1.9837 ± 0.0005
After Zn 200	4.6136 ± 0.0001	1.6658 ± 0.0001
After Zn 400	4.6136 ± 0.0001	1.7027 ± 0.0002
mse (initial-after Cu 200)	0.0019	0.0326
mse (initial-after Cu 400)	0.0019	0.2613
mse (initial-after Zn 200)	0.0038	0.0374
mse (initial-after Zn 400)	0.0038	0.0530
% increase (after Cu 400-after Cu 200)	0.0	**20.0 $\pm$ 1.0**
% increase (after Zn 400-after Zn 200)	0.0	**2.2 $\pm$ 0.3**

Figure 6 shows the approximation of cumulative infiltration experimental points of sandy soil (S) with G&A and P models, for the five cases: (a) initial (before contaminating the soil column with the Cu and Zn solutions) (b) after contaminating with Cu 200 mg·L^{-1} solution (Cu 200) (c) after contaminating with Cu 400 mg·L^{-1} solution (Cu 400) (d) after contaminating with Zn 200 mg·L^{-1} solution (Zn 200) and (e) after contaminating with Zn 400 mg·L^{-1} solution (Zn 400).
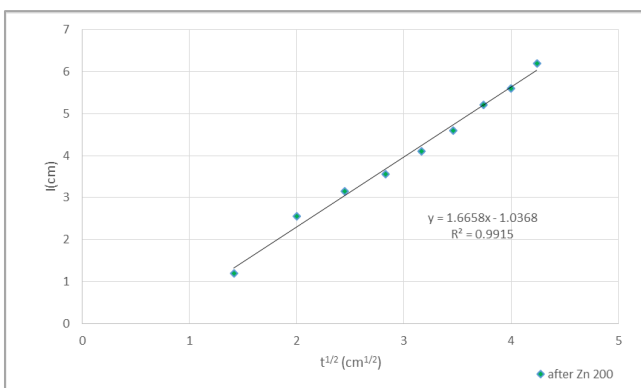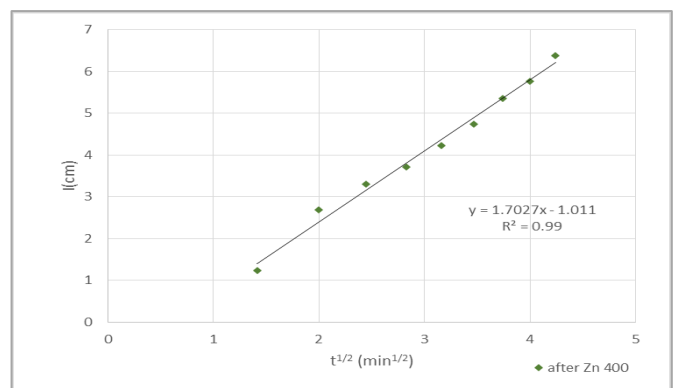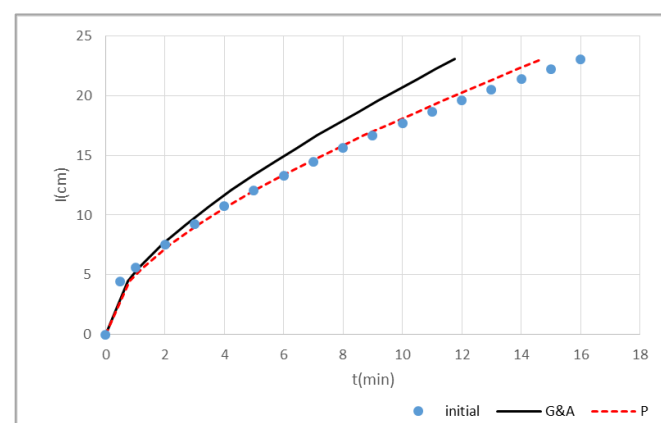
In Figure 7, the cumulative infiltration experimental points of loamy clay soil (LC), for the 5 cases (a) initial, (b) after Cu 200, (c) Cu 400, (d) Zn 200 and (e) Zn 400 contamination), were approximated with G&A and P models.

Table 5 shows the relative mse between G&A model and the experimental points, as well as the P model and the experimental points of cumulative infiltration after contaminating with Cu 200 mg·L^{-1} solution (Cu 200), after contaminating with Cu 400 mg·L^{-1} solution (Cu 400), after contaminating with Zn 200 mg·L^{-1} solution (Zn 200) and after contaminating with Zn 400 mg·L^{-1} solution (Zn 400), for sandy (S) and loamy clay (LC) soil.

(**a**)

Figure 6. *Cont.*

(b)
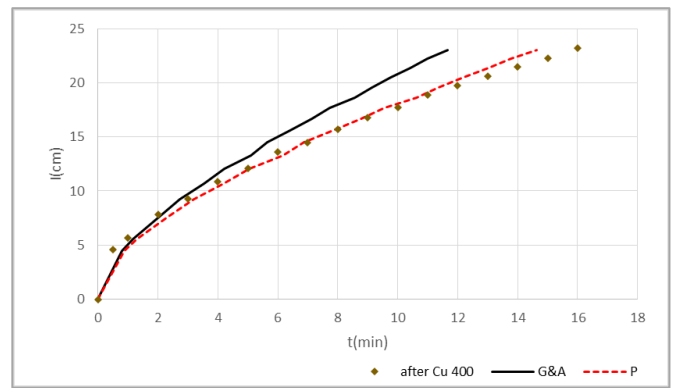
(c)
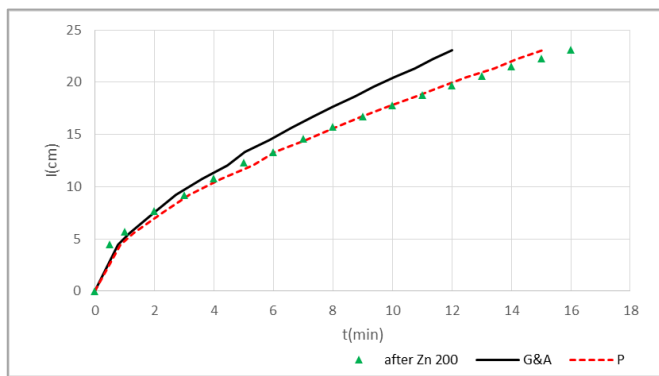
(d)
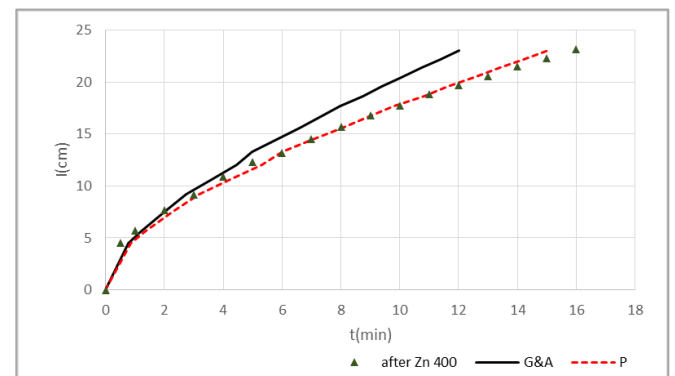
(e)

Figure 6. Approximation of cumulative infiltration experimental points of sandy soil (S) with G&A and P models, for the five cases: (**a**) initial (before contaminating the soil column with the Cu and Zn solutions) (**b**) after contaminating with Cu 200 mg·L^{-1} solution (Cu 200) (**c**) after contaminating with Cu 400 mg·L^{-1} solution (Cu 400) (**d**) after contaminating with Zn 200 mg·L^{-1} solution (Zn 200) and (**e**) after contaminating with Zn 400 mg·L^{-1} solution (Zn 400) (*n* = 2).

(a)

Figure 7. *Cont.*

(**b**)

(**c**)

(**d**)

(**e**)
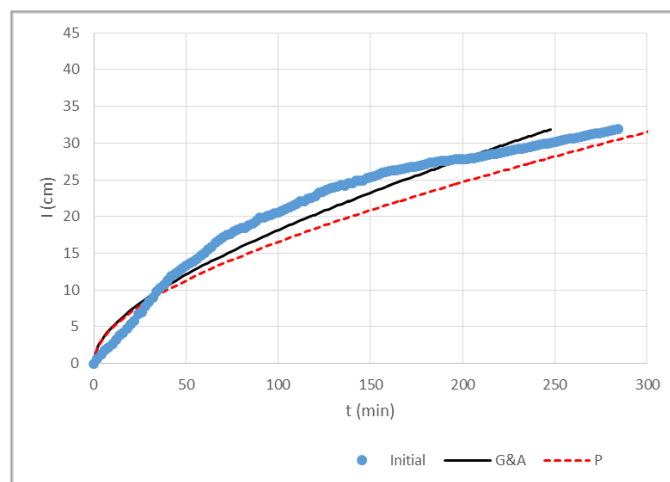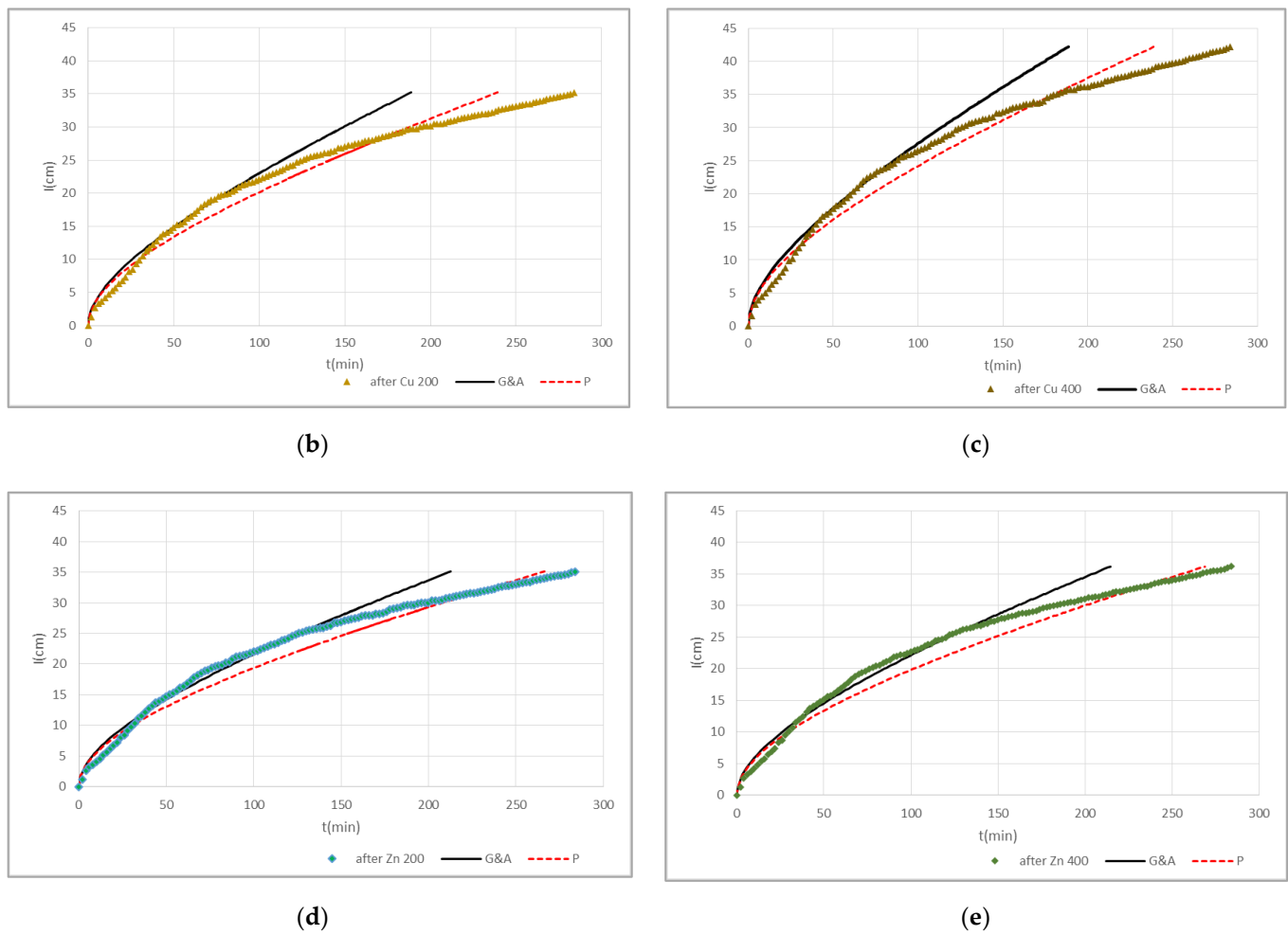
Figure 7. Approximation of cumulative infiltration experimental points of loamy clay (LC) soil with G&A and P models, for the five cases: (**a**) initial (before contaminating the soil column with the Cu and Zn solutions) (**b**) after contaminating with Cu 200 mg·L^{-1} solution (Cu 200) (**c**) after contaminating with Cu 400 mg·L^{-1} solution (Cu 400) (**d**) after contaminating with Zn 200 mg·L^{-1} solution (Zn 200) and (**e**) after contaminating with Zn 400 mg·L^{-1} solution (Zn 400) (*n* = 2).
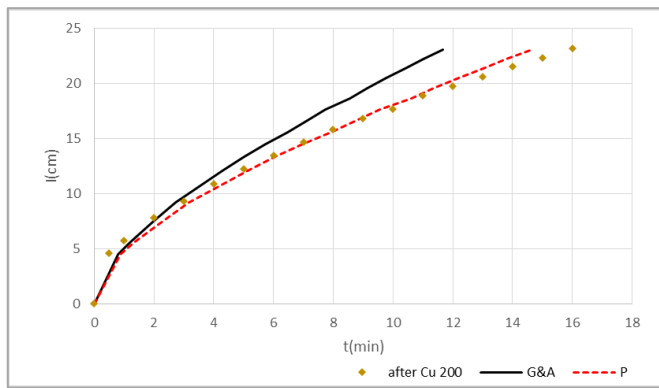
Table 5. Relative mse between G&A model and experimental points and P model and experimental points of cumulative infiltration after contaminating with Cu 200 mg·L^{-1} solution (Cu 200), after contaminating with Cu 400 mg·L^{-1} solution (Cu 400), after contaminating with Zn 200 mg·L^{-1} solution (Zn 200) and after contaminating with Zn 400 mg·L^{-1} solution (Zn 400), for sandy (S) and loamy clay (LC) soil (*n* = 2).

	S		**LC**	
	Relative mse (G&A-exper. Points)	**Relative mse (P-exper. Points)**	**Relative mse (G&A-exper. Points)**	**Relative mse (P-exper. Points)**
Initial	0.05	0.03	0.10	0.14
After Cu 200	0.06	0.04	0.06	0.05
After Cu 400	0.06	0.04	0.03	0.03
After Zn 200	0.05	0.04	0.07	0.05
After Zn 400	0.05	0.04	0.04	0.04

4. Discussion

The soil samples exhibited alkaline characteristics ($pH_{(S)}$ = 7.4, $pH_{(LC)}$ = 7.6). The loamy clay soil contained 5.1% organic matter content (OM), while the sandy soil sample contained no detectable OM content. Background Cu and Zn concentrations at the soil samples were not detectable, so both soils were considered as "not polluted". Sandy soil showed a negligible adsorption of Cu and Zn, while doubling Cu and Zn concentrations exerted no further impact on the adsorption capacity of sand. On the other hand, loamy clay soil showed a different behavior, as the remaining values of Cu and Zn cations were increased by 29% and 7%, respectively, after doubling Cu and Zn concentrations in the inflow solution.

At sandy soil, infiltration data showed no significant difference after the pollution with Cu and Zn cations, in all cases. Doubling concentrations did not exert any impact on the infiltration process, nor on hydraulic conductivity, derivative dI/dt and sorptivity. Contrarily, the 29% increase in the adsorption of Cu, after doubling Cu concentration, led to an average 19.9% increase in the cumulative infiltration experimental points at loamy clay soil. According to our findings, doubling the Zn concentration led to an average 3.1% increase in infiltration points (Table 2). Kabata-Pendias (2011) and Alloway et al. (2013) noticed that zinc mobility is greater than copper mobility, as copper is strongly retained by the soil solid phase. Sandy soils showed low holding heavy metal capacity, which could cause either high heavy metal uptake at crops or heavy metal leaching in the lower soil layers [56]. According to our findings, solutions of Cu and Zn did not affect the hydraulic properties of the sandy soil, due to the negligible adsorption capacity of sandy soil. On the other hand, the presence of Cu and Zn cations in the incoming fluid affected cumulative infiltration, hydraulic conductivity, infiltration rate and sorptivity of loamy clay soil. Moreover, doubling the concentration of Cu in the incoming fluid led to a 29% increase in the Cu adsorption; this behavior also led to a direct influence of the hydraulic parameters. Thus, we noticed a roughly 20% increase in all hydraulic parameters of loamy clay soil. On the other hand, doubling the concentration of Zn in the incoming fluid affected the adsorption by 7% (increase), while the effect on hydraulic parameters varied from 2.2% to 3.1%.

According to Equation (2), the increase in K_s leads to an increase in S, which was confirmed experimentally in all cases. As loamy clay soil is a cohesive soil, it exhibits low initial hydraulic conductivity and infiltration rate [30]. Ponded with Cu and Zn solutions singly, the presence of each heavy metal improved hydraulic conductivity, as well as the infiltration process. This may have occurred because of both active clay minerals and the alkaline pH, which confers to loamy clay soil a higher ability to retain Cu and Zn cations [29,57]. The environment is strongly influenced by the soil structure, while soil structure is regularly expressed as aggregate stability degree [27]. The particle cementation, rearrangement and flocculation exert an essential impact on aggregation or the aggregate stability degree, as well as fixation [28], which is enhanced mostly by soil organic carbon (SOC), carbonates, bridges of ions, and clay particles. Aggregation could be either enhanced or weakened by the complicated interactions of the aggregates. Aggregation is associated with clay-size particles that rearrange and flocculate, but swelling clay can cause aggregate rupture [30]. Organometallic compounds along with cations act as bridges between the soil particles. SOC sources are mostly the animals and plants residues [28]; the aggregation enhances the SOC concentration into the soil. The effectiveness of SOC in fixation and aggregation is linked to its decomposition rate, which is affected by the physical and chemical protection from microbial action [30]. Aggregation is enhanced by the precipitation of hydroxides, carbonates and phosphates. Ca^{2+}, Si^{4+}, Al^{3+} and Fe^{3+} induce the precipitation of compounds, which play a significant role in bonding with primal particles. Plant's radicals and hyphae may lead to aggregation of particles, while the repositioning of the particles and the release of organic compounds strengthen aggregation further [58]. Agricultural practices along with environmental changes often lead to soil structure modification. Any practice which increases productivity, while, at the same time,

decreases soil disruption, is beneficial to structural development and aggregation [59]. Copper makes strong bonds with fine clay particles and organic matter. In addition, after removing the organic matter, retention of Cu by fine clay is increased in comparison to coarse and medium clay, while the adsorption of Cu and Zn increase above values of pH 4 and 5, respectively [29]. Metals entering into the soil due to contact with the atmospheric air, due to infiltration, interact with the clay and organic particles and accumulate into the soil [58]. Previous studies have noted that soil aggregate-size allocation is influenced by heavy metal concentrations into the soil, while higher concentrations of heavy metals have been found in fine particles of surface soils. Higher organic matter, higher clay contents, larger surface, along with the presence of Fe single bond Mn oxide phases, are responsible for the higher heavy metal concentrations [44]. It's also been reported that the significant impact of soil organic matter in the retention and the leaching of heavy metals in soil aggregates [60,61]. Consequently, the presence of Cu and Zn cations may have interacted with clay particles, affecting aggregation and soil structure in loamy clay soil. This behavior led to improved infiltration rate, hydraulic conductivity and sorptivity of loamy clay soil. Furthermore, all hydraulic parameters under investigation, increased by 20% and ~3%, after doubling Cu and Zn concentrations in the inflow solution (while adsorption of Cu and Zn increased 29% and 7% respectively). On the other hand, in the case of sandy soil, no significant changes on hydraulic parameters were obtained, due to low % values of clay particles [40].

Approximation of experimental points with G&A and P infiltration models showed very good agreement of both models with the infiltration data. There were no significant differences between the behaviors of the two models. However it is remarkable that in the case of loamy clay soil, the differences in hydraulic properties lead to decrease of the relative mean square error between the models and the experimental data, which is consistent with previous studies, indicating that the relative error becomes smaller as the soil becomes less fine [10,62]. Thus, G&A and P models satisfactorily simulate the experimental points and they have captured the changes at the hydraulic parameters.

Development of desirable soil structure improves porosity, reduces corrosion and improves field capacity, root filtration and ease of cultivation. High levels of clay are often linked with contaminated soils, so improving permeability and infiltration rate is a necessity. Concentrations of Cu and Zn above 200 mg·L^{-1} in the incoming fluid can lead to enhanced soil structure of loamy clay soils. Leaching of metals in the deeper layers of the loamy clay soil profile could be avoided, due to the adsorption of copper and zinc cations by clay particles.

5. Conclusions

Two different soil types were used in order to investigate the impact of Cu and Zn cations on their hydraulic properties. Hydraulic conductivity, cumulative infiltration, sorptivity and infiltration rate were estimated before and after the contamination of the soil samples, in the laboratory under artificial ponding irrigation. Two different (doubled) concentrations of Cu were used in order to contaminate the sandy and the loamy clay soil samples and the same procedure was followed in the case of Zn. At loamy clay soil, doubling Cu concentration, from 200 mg·L^{-1} to 400 mg·L^{-1} into the incoming solution, led to raise of adsorption by 29%. By doubling Zn concentration from 200 mg·L^{-1} to 400 mg·L^{-1}, adsorption was increased by 7%. Hydraulic conductivity, sorptivity, along with infiltration rate, were increased by about 20% after doubling the concentration of Cu in the incoming solution, while in the case of Zn, the hydraulic properties were increased by values between 2.2% and 3%. In the case of loamy clay soil, the increase in the positive charge in the incoming fluid increased the adsorption capacity of the soil and the amount of the aggregates, which led accordingly to improved soil structure, while in sandy soil, due to the absence of clay particles, the increase in the heavy metal concentration exerted no impact on aggregation and soil structure. Thus, polluted loamy clay soils with Cu (or Zn), may show improved soil structure and an increased infiltration rate, which was

also indicated by the G&A and P models simulation. Further investigation of the environmental parameters that influence the mobility/immobilization of metal cations could be a challenging accomplishment.

Author Contributions: Conceptualization A.A. and E.E.G.; methodology, A.A. and E.E.G.; software, A.A., P.S. and E.E.G.; validation, A.A. and E.E.G.; formal analysis, A.A., A.D., P.S. and E.E.G.; investigation, A.A. and E.E.G.; resources A.A. and E.E.G.; data curation, A.A., A.D., P.S. and E.E.G.; writing—original draft preparation, A.A.; writing—review and editing, A.A. and E.E.G.; visualization, A.A. and E.E.G.; supervision, A.A. and E.E.G.; project administration, A.A. and E.E.G. conceived the idea of the research and designed the experimental procedure. A.A. processed the data and wrote the article. P.S. contributed to data analyses and E.E.G. wrote the sections involving heavy metals, soil science and reviewed the article. A.D. carried out the experimental procedure as part of his graduate thesis, under A.A. and E.E.G. supervision. All authors have read and agreed to the published version of the manuscript.

Funding: This research received no external funding.

Informed Consent Statement: Not applicable.

Data Availability Statement: Data available on request due to restrictions e.g., privacy or ethical. The data presented in this study are available on request from the corresponding author. The data are not publicly available due to privacy and copyright reasons.

Conflicts of Interest: The authors declare no conflict of interest.

References

1. Rousseva, S.; Kercheva, M.; Shishkov, T.; Lair, G.J.; Nikolaidis, N.P.; Moraetis, D.; Krám, P.; Bernasconi, S.M.; Blum, W.E.H.; Menon, M.; et al. Chapter Two: Soil water characteristics of European SoilTrEC critical zone observatories. In *Advances in Agronomy*; Elsevier: Amsterdam, The Netherlands, 2017; Volume 142, pp. 29–72.
2. Wanniarachchi, D.; Cheema, M.; Thomas, R.; Kavanagh, V.; Galagedara, L. Impact of soil amendments on the hydraulic conductivity of boreal agricultural podzols. *Agriculture* **2019**, *9*, 133. [CrossRef]
3. Li, Z.; Liu, H.; Zhao, W.; Yang, Q.; Yang, R.; Liu, J. Estimation of evapotranspiration and other soil water budget components in an irrigated agricultural field of a desert oasis, using soil moisture easurements. *Hydrol. Earth Syst. Sci.* **2018**, 1–17. [CrossRef]
4. Sihag, P.; Esmaeilbeiki, F.; Singh, B.; Ebtehaj, I.; Bonakdari, H. Modeling unsaturated hydraulic conductivity by hybrid soft computing techniques. *Soft Comput.* **2019**, *23*, 12897–12910. [CrossRef]
5. Guellouz, L.; Askri, B.; Jaffré, J.; Bouhlila, R. Estimation of the soil hydraulic properties from field data by solving an inverse problem. *Sci. Rep.* **2020**, *10*, 9359. [CrossRef]
6. Gallage, C.; Kodikara, J.; Uchimura, T. Laboratory measurement of hydraulic conductivity functions of two unsaturated sandy soils during drying and wetting processes. *Soils Found.* **2013**, *53*, 417–430. [CrossRef]
7. Ali, A.; Biggs, A.J.W.; Marchuk, A.; Bennett, J.M. Effect of irrigation water pH on saturated hydraulic conductivity and electrokinetic properties of acidic, neutral, and alkaline soils. *Soil Sci. Soc. Am. J.* **2019**, *83*, 1672–1682. [CrossRef]
8. Singh, B.; Sihag, P.; Parsaie, A.; Angelaki, A. Comparative analysis of artificial intelligence techniques for the prediction of infiltration process. *Geol. Ecol. Landsc.* **2020**, *5*, 109–118. [CrossRef]
9. Wang, X.; Zhao, Y.; Liu, H.; Xiao, W.; Chen, S. Evaluating the water holding capacity of multilayer soil profiles using hydrus-1d and multi-criteria decision analysis. *Water* **2020**, *12*, 773. [CrossRef]
10. Angelaki, A.; Sakellariou-Makrantonaki, M.; Tzimopoulos, C. Theoretical and experimental research of cumulative infiltration. *Transp. Porous Media* **2013**, *100*, 247–257. [CrossRef]
11. Sihag, P.; Singh, B.; Sepah Vand, A.; Mehdipour, V. Modeling the infiltration process with soft computing techniques. *ISH J. Hydraul. Eng.* **2018**, *26*, 138–152. [CrossRef]
12. Vand, A.S.; Sihag, P.; Singh, B.; Zand, M. Comparative evaluation of infiltration models. *KSCE J. Civ. Eng.* **2018**, *22*, 4173–4184. [CrossRef]
13. Pandey, P.K.; Pandey, V. Estimation of infiltration rate from readily available soil properties (RASPs) in fallow cultivated land. *Sustain. Water Resour. Manag.* **2019**, *5*, 921–934. [CrossRef]
14. Poulovassilis, A.; Elmaloglou, S.; Kerkides, P.; Argyrokastritis, I. A variable sorptivity infiltration equation. *Water Resour. Manag.* **1989**, *3*, 287–298. [CrossRef]
15. Argyrokastritis, I.; Kerkides, P. A note to the variable sorptivity infiltration equation. *Water Resour. Manag.* **2003**, *17*, 133–145. [CrossRef]
16. Evangelides, C.; Arampatzis, G.; Tzimopoulos, C. Estimation of soil moisture profile and diffusivity using simple laboratory procedures. *Soil Sci.* **2010**, *175*, 118–127. [CrossRef]

17. Angelaki, A.; Sihag, P.; Sakellariou-Makrantonaki, M.; Tzimopoulos, C. The effect of sorptivity on cumulative infiltration. *Water Sci. Technol. Water Supply* **2021**, *21*, 606–614. [CrossRef]

18. Rahmati, M.; Vanderborght, J.; Simunek, J.; Vrugt, J.A.; Moret-Fernandez, D.; Latorre, B.; Lassabatere, L.; Vereecken, H. Soil hydraulic properties estimation from one-dimensional infiltration experiments using characteristic time concept. *Vadose Zone J.* **2020**, *19*, e20068. [CrossRef]

19. Poulovassilis, A.; Argyrokastritis, I. A new approach for studying vertical infiltration. *Soil Res.* **2020**, *58*, 509–518. [CrossRef]

20. Green, W.H.; Al, E. Studies of soil physics: The flow of air and water through soils. *J. Agric. Sci.* **1911**, *4*, 11–24.

21. Richards, A.L. Capillary conduction of liquids through porous medium. *Physics* **1931**, *1*, 318–333. [CrossRef]

22. Parlange, J.Y.; Barry, D.A.; Haverkamp, R. Explicit infiltration equations and the Lambert W-function. *Adv. Water Resour.* **2002**, *25*, 1119–1124. [CrossRef]

23. Wang, K.; Yang, X.; Liu, X.; Liu, C. A simple analytical infiltration model for short-duration rainfall. *J. Hydrol.* **2017**, *555*, 141–154. [CrossRef]

24. Chen, S.; Mao, X.; Wang, C. A modified green-ampt model and parameter determination for water infiltration in fine-textured soil with coarse interlayer. *Water* **2019**, *11*, 787. [CrossRef]

25. Liu, Z.-Z.; Yan, Z.-X.; Qiu, Z.-H.; Wang, X.-G.; Li, J.-W. Stability analysis of an unsaturated soil slope considering rainfall infiltration based on the Green-Ampt model. *J. Mt. Sci.* **2020**, *17*, 2577–2590. [CrossRef]

26. Tzimopoulos, C.; Papaevangelou, G.; Papadopoulos, K.; Evangelidis, C. New explicit form of green and ampt model for cumulative infiltration estimation. *Res. J. Environ. Sci.* **2019**, *14*, 30–41. [CrossRef]

27. Sparks, D.L. Toxic metals in the environment: The role of surfaces. *Elements* **2005**, *1*, 193–197. [CrossRef]

28. Kabata-Pendias, A. *Trace Elements in Soils and Plants: Fourth Edition*; CRC Press; Taylor and Francis Group: Ann Arbor, MI, USA, 2011; ISBN 9781420093704.

29. Liu, L.; Li, W.; Song, W.; Guo, M. Remediation techniques for heavy metal-contaminated soils: Principles and applicability. *Sci. Total Environ.* **2018**, *633*, 206–219. [CrossRef]

30. Alloway, B.J. *Heavy Metals in Soils: Trace Metals and Metalloids in Soils and Their Bioavailability*, 3rd ed.; Alloway, B.J., Ed.; Blackie Academic and Professional: London, UK, 2013; ISBN 9789400744691.

31. Berkowitz, B.; Dror, I.; Yaron, B. Sorption, retention, and release of contaminants. In *Contaminant Geochemistry: Transport and Fate in the Subsurface Environment*; Berkowitz, B., Dror, I., Yaron, B., Eds.; Springer: Heidelberg/Berlin, Germany, 2008; pp. 93–126.

32. Golia, E.E.; Dimirkou, A.; Floras, S.A. Spatial monitoring of arsenic and heavy metals in the Almyros area, Central Greece. Statistical approach for assessing the sources of contamination. *Environ. Monit. Assess.* **2015**, *187*, 399–412. [CrossRef]

33. Oorts, K. Copper. In *Heavy Metals in Soils. Environmental Pollution*; Springer: Dordrecht, The Netherlands, 2013; pp. 367–394.

34. Khanam, R.; Kumar, A.; Nayak, A.K.; Shahid, M.; Tripathi, R.; Vijayakumar, S.; Bhaduri, D.; Kumar, U.; Mohanty, S.; Panneerselvam, P.; et al. Metal(loid)s (As, Hg, Se, Pb and Cd) in paddy soil: Bioavailability and potential risk to human health. *Sci. Total Environ.* **2020**, *699*, 134330. [CrossRef]

35. Bourazanis, G.; Katsileros, A.; Kosmas, C.; Kerkides, P. The effect of treated municipal wastewater and fresh water on saturated hydraulic conductivity of a clay-loamy soil. *Water Resour. Manag.* **2016**, *30*, 2867–2880. [CrossRef]

36. Markiewicz-Patkowska, J.; Hursthouse, A.; Przybyla-Kij, H. The interaction of heavy metals with urban soils: Sorption behaviour of Cd, Cu, Cr, Pb and Zn with a typical mixed brownfield deposit. *Environ. Int.* **2005**, *31*, 513–521. [CrossRef] [PubMed]

37. Nartowska, E.; Kozlowski, T.; Gawdzik, J. Assessment of the influence of copper and zinc on the microstructural parameters and hydraulic conductivity of bentonites on the basis of SEM tests. *Heliyon* **2019**, *5*, e02142. [CrossRef] [PubMed]

38. Kozlowski, T.; Walaszczyk, L.; Kurpias-Warianek, K. Application of SEM to analysis of permeability coefficient of cohesive soils. *Arch. Hydro-Eng. Environ. Mech.* **2011**, *58*, 47–64. [CrossRef]

39. Baghernejad, M.; Javaheri, F.; Moosavi, A.A. Adsorption isotherms of copper and zinc in clay minerals of calcareous soils and their effects on X-ray diffraction. *Arch. Agron. Soil Sci.* **2015**, *61*, 1061–1077. [CrossRef]

40. Kypritidou, Z.; Argyraki, A. Geochemical interactions in the trace element–soil–clay system of treated contaminated soils by Fe-rich clays. *Environ. Geochem. Health* **2020**, *43*, 2483–2503. [CrossRef]

41. Xie, S.; Wen, Z.; Zhan, H.; Jin, M. An Experimental Study on the Adsorption and Desorption of Cu(II) in Silty Clay. *Geofluids* **2018**, *2018*, 3610921. [CrossRef]

42. Cui, H.; Ma, K.; Fan, Y.; Peng, X.; Mao, J.; Zhou, D.; Zhang, Z.; Zhou, J. Stability and heavy metal distribution of soil aggregates affected by application of apatite, lime, and charcoal. *Environ. Sci. Pollut. Res.* **2016**, *23*, 10808–10817. [CrossRef]

43. Gao, X.; Gu, Y.; Xie, T.; Zhen, G.; Huang, S.; Zhao, Y. Characterization and environmental risk assessment of heavy metals in construction and demolition wastes from five sources (chemical, metallurgical and light industries, and residential and recycled aggregates). *Environ. Sci. Pollut. Res.* **2015**, *22*, 9332–9344. [CrossRef]

44. Xiao, R.; Zhang, M.; Yao, X.; Ma, Z.; Yu, F.; Bai, J. Heavy metal distribution in different soil aggregate size classes from restored brackish marsh, oil exploitation zone, and tidal mud flat of the Yellow River Delta. *J. Soils Sediments* **2016**, *16*, 821–830. [CrossRef]

45. Deng, A.; Wang, L.; Chen, F.; Li, Z.; Liu, W.; Liu, Y. Soil aggregate-associated heavy metals subjected to different types of land use in subtropical China. *Glob. Ecol. Conserv.* **2018**, *16*, e00465. [CrossRef]

46. Defera, J.; Wogi, L.; Mishra, B.B. Assessment of physicochemical properties of soil under different land use types at Wuy Gose Sub-Watershed, North Shoa Zone of Oromia Region, Ethiopia. *Int. J. Agric. Biol. Sci.* **2019**, 34–58.

47. Nartowska, E. The effects of potentially toxic metals (copper and zinc) on selected physical and physico-chemical properties of bentonites. *Heliyon* **2019**, *5*, e02563. [CrossRef] [PubMed]

48. Williams, S. *Official Method of Analysis*, 14th ed.; Association of Official Chemists, Inc.: Arlington, VA, USA, 1984; Volume 6, ISBN 9788578110796.

49. Page, A.L. Methods of soil analysis-Part 2: Chemical and Microbiological properties. (2nd edition). *Am. Soc. Agron. Inc. Publ. Madison USA* **1982**, *9*, 421–422.

50. *ISO/DIS 11466*; Environment Soil Quality. ISO Standards Compendium. International Organization for Standardization: Geneva, Switzerland, 1994.

51. Golia, E.E.; Tsiropoulos, N.G.; Dimirkou, A.; Mitsios, I. Distribution of heavy metals of agricultural soils of central Greece using the modified BCR sequential extraction method. *Int. J. Environ. Anal. Chem.* **2007**, *87*, 1053–1063. [CrossRef]

52. Van der Lee, J.J.; Temminghoff, F.; Houba, V.J.G.; Novozamsky, I. Background corrections in the determination of Cd and Pb by flame AAS in plant and soil samples with high Fe levels. *Appl. Spectrosc.* **1987**, *41*, 388–390. [CrossRef]

53. Lajunen, L.H.G. Spectrochemical analysis by atomic absorption and emission. In *Analytica Chimica Acta*; The Royal Society Chemistry: Cambridge, UK, 1992.

54. ASTM D5084-10 Standard test methods for measurement of hydraulic conductivity of saturated porous materials using a flexible wall permeameter. *Annu. B ASTM Stand.* **2010**, 1–23. [CrossRef]

55. Sakellariou-Makrantonaki, M.; Angelaki, A.; Evangelides, C.; Bota, V.; Tsianou, E.; Floros, N. Experimental determination of hydraulic conductivity at unsaturated soil column. *Proc. Procedia Eng.* **2016**, *162*, 83–90. [CrossRef]

56. Volk, J.; Yerokun, O. Effect of application of increasing concentrations of contaminated water on the different fractions of Cu and Co in sandy loam and clay loam soils. *Agriculture* **2016**, *6*, 64. [CrossRef]

57. Golia, E.E.; Tsiropoulos, G.N.; Füleky, G.; Floras, S.; Vleioras, S. Pollution assessment of potentially toxic elements in soils of different taxonomy orders in central Greece. *Environ. Monit. Assess.* **2019**, *191*, 106. [CrossRef]

58. Lasota, J.; Blonska, E.; Lyszczarz, S.; Tibbett, M. Forest humus type governs heavy metal accumulation in specific organic matter fractions. *Water. Air. Soil Pollut.* **2020**, *231*, 80. [CrossRef]

59. Bronick, C.J.; Lal, R. Soil structure and management: A review. *Geoderma* **2005**, *124*, 3–22. [CrossRef]

60. Li, Z.; Huang, B.; Huang, J.; Chen, G.; Zhang, C.; Nie, X.; Luo, N.; Yao, H.; Ma, W.; Zeng, G. Influence of removal of organic matter and iron and manganese oxides on cadmium adsorption by red paddy soil aggregates. *RSC Adv.* **2015**, *5*, 90588–90595. [CrossRef]

61. Liu, Y.; Liu, W.; Wu, L.; Liu, C.; Wang, L.; Chen, F.; Li, Z. Soil aggregate-associated organic carbon dynamics subjected to different types of land use: Evidence from 13C natural abundance. *Ecol. Eng.* **2018**, *122*, 295–302. [CrossRef]

62. Selker, J.S.; Assouline, S. An explicit, parsimonious, and accurate estimate for ponded infiltration into soils using the Green and Ampt approach. *Water Resour. Res.* **2017**, *53*, 7481–7487. [CrossRef]